PROCEEDINGS of the
23rd International Congress on Acoustics
9 to 13 September 2019 in Aachen, Germany

Assessing the similitude of vibrating plates

Christian ADAMS[(1)], Joachim BÖS[(1)], Tobias MELZ[(1),(2)]

[(1)]Technische Universität Darmstadt, research group System Reliability, Adaptive Structures, and Machine Acoustics SAM, Darmstadt, Germany, adams@sam.tu-darmstadt.de

[(2)]Fraunhofer Institute for Structural Durability and System Reliability LBF, Darmstadt, Germany

Abstract

The similitude of vibrating structures allows for transferring vibration responses from a scaled structure to an original structure using scaling laws. Numerical calculations and experimental measurements show that complete similitude conditions such as equal damping and geometrically complete similitude are essential to accurately transfer vibration responses from small-scaled structures to the original structure or vice versa. However, complete similitude conditions can hardly be achieved in practice. A different damping or geometrical distortions cause the mode shape order to change, which leads to errors when using scaling laws. Nevertheless, the scaling laws can transfer the vibration responses from the scaled structure to the original structure with a sufficient accuracy in some cases. This paper analyzes vibration responses of rectangular plates with various sizes. The vibration responses are obtained from laser DOPPLER vibrometry, and the loss factors are obtained from transfer function measurements. The vibration responses of an original rectangular plate is transferred to several scaled rectangular plates. The accuracy of the transferred vibration responses is assessed by comparing them with the measured vibration responses of the scaled rectangular plates, where several measures are used in order to assess how well the vibration responses agree.

Keywords: similitude, vibrations, rectangular plates, laser DOPPLER vibrometry

1 INTRODUCTION

Similitude analyses allow for deriving scaling laws, which are used to transfer vibration responses from scaled structures to an original structure or vice versa. Scaling laws for vibrating structures have been introduced in several papers. A review paper written by CASABURO [1] summarizes scaling methods for structural design engineering, where similitude analysis is reviewed with respect to methods to derive scaling laws, structures used in similitude analyses, and applications of similitude analysis methods in various engineering subjects. It is shown that – despite the fact that similitude analysis has a long history in engineering – incomplete similitude conditions still limit the application of scaling laws in practice. In vibroacoustics, incomplete similitude conditions arise from a different damping of the original structure and of the scaled ones and from geometrically incomplete similitude. Thus, the limitations of scaling laws need to be elaborated, which requires appropriate measures to assess the accuracy of scaled vibration responses.

This paper shows how incomplete similitude conditions due to the damping and due to geometrically incomplete similitude affects the accuracy of scaled vibration responses. A vibrating rectangular plate is used as a representative example. A frequency response analysis is carried out for each rectangular plate using a scanning laser DOPPLER vibrometer (SLDV), and the loss factors are obtained from frequency response function measurements. The vibration responses of an original rectangular plate are transferred to several scaled rectangular plates using scaling laws, which are derived from numerical calculations using the method proposed in [2, 3]. The similitude of the rectangular plates is assessed by several measures that describe how well the transferred vibration responses agree with the measured ones.

2 FUNDAMENTALS

This section introduces the scaling laws that are used to transfer (hereafter referred to as *to replicate*) the vibration responses of the original rectangular plate to the scaled rectangular plates. The measures that are used to assess the similitude are introduced as well.

2.1 Scaling laws of vibrating rectangular plates

The scaling laws are derived provided that the rectangular plates are in complete similitude. In a next step, the scaling laws are enhanced towards geometrically incomplete similitude. In order to clearly identify the rectangular plates, the following notation is used:

- parent: original rectangular plate with known vibration responses. These vibration responses are used to replicate the vibration responses of the scaled rectangular plates.
- replica: scaled rectangular plate in complete similitude. Its vibration responses are estimated using scaling laws.
- avatar: scaled rectangular plate in incomplete similitude. Its vibration responses are estimated using scaling laws.

The scaling laws are derived for the rectangular plates' mean squared transfer admittance (MSTA), which is defined as

$$Sh_{\mathrm{T}}^2(f) = S\frac{\overline{\tilde{v}^2}(f)}{\tilde{F}^2(f)}. \tag{1}$$

S, $\overline{\tilde{v}^2}(f)$, and $\tilde{F}^2(f)$ denote the vibrating surface area, the surface-averaged squared RMS[1] vibration velocity, and the squared RMS excitation force, respectively. f denotes the frequency. It is assumed that the rectangular plates are scaled in their geometrical dimensions, i.e., length a, width b, and thickness t. Next, the scaling factors

$$\phi_a = \frac{a^{(\mathrm{r})}}{a^{(\mathrm{p})}} = \phi_b = \frac{b^{(\mathrm{r})}}{b^{(\mathrm{p})}} = \phi_l \text{ and } \phi_t = \frac{t^{(\mathrm{r})}}{t^{(\mathrm{p})}} \tag{2}$$

for length, width, and thickness are introduced, respectively. The superscript (p) denotes the parent and the superscript (r) a replica. Complete similitude conditions require ϕ_a and ϕ_b to be equal. Applying the scaling method from [2, 3] yields

$$\frac{Sh_{\mathrm{T}}^{2(\mathrm{r})}(f^{(\mathrm{r})})}{Sh_{\mathrm{T}}^{2(\mathrm{p})}(f^{(\mathrm{p})})} = \phi_{Sh} = \phi_l^2\phi_t^{-4} \tag{3}$$

for the MSTA, where the frequencies are scaled by

$$\frac{f^{(\mathrm{r})}}{f^{(\mathrm{p})}} = \phi_f = \phi_l^{-2}\phi_t^1. \tag{4}$$

In order to enhance the scaling laws to geometrically incomplete similitude, the scaling factor ϕ_l in Eqs. (3) and (4) is substituted by

$$\phi_l = \frac{1}{2}(\phi_a + \phi_b). \tag{5}$$

Thus, the vibration responses of avatars in geometrically incomplete similitude are obtained from another replica that is as close as possible to the avatar [5].

[1] RMS: root mean square

2.2 Similitude measures

Three measures are introduced that are used to asses how well the replicated MSTA matches the measured MSTA of replicas (and avatars):

- the HAUSDORFF distance [8], which is used in [9] to assess the similitude of vibrating rectangular plates,
- the MAHALANOBIS distance [10], which is introduced in [3] to assess the similitude of vibrating rectangular plates, and
- the frequency response function similarity metric (FRFSM), which is introduced by LEE [11].

The HAUSDORFF distance of two (arbitrary) frequency response functions $\mathbf{A} = \{a_1, a_2, \ldots, a_N\}$ and $\mathbf{B} = \{b_1, b_2, \ldots, b_M\}$ is defined as

$$d_{\mathrm{H}} = \max\left(d'_{\mathrm{H}}(\mathbf{A},\mathbf{B}), d'_{\mathrm{H}}(\mathbf{B},\mathbf{A})\right), \tag{6}$$

where $d'_{\mathrm{H}}(\mathbf{A},\mathbf{B})$ and $d'_{\mathrm{H}}(\mathbf{B},\mathbf{A})$ are the unidirectional HAUSDORFF distances

$$d'_{\mathrm{H}}(\mathbf{A},\mathbf{B}) = \max_{a\varepsilon\mathbf{A}} \min_{b\varepsilon\mathbf{B}} \|a-b\|_2 \quad \text{and} \quad d'_{\mathrm{H}}(\mathbf{B},\mathbf{A}) = \max_{b\varepsilon\mathbf{B}} \min_{a\varepsilon\mathbf{A}} \|a-b\|_2, \tag{7}$$

of these frequency response functions. $\|\cdot\|_2$ denotes the EUCLIDEAN norm [8]. The HAUSDORFF distance can be seen as the maximum distance of minimum distances between the two frequency response functions, thus, describing the maximum mismatch between $\mathbf{A}$ and $\mathbf{B}$ [8].

The MAHALANOBIS distance is similar to a EUCLIDEAN distance that is weighted by the inverse of the covariance matrix Σ^{-1}. Taking again (arbitrary) frequency response functions $\mathbf{A}$ and $\mathbf{B}$, the MAHALANOBIS distance yields

$$d_{\mathrm{M}}(\mathbf{A},\mathbf{B}) = \sqrt{(\mathbf{A}-\mathbf{B})^T \Sigma^{-1} (\mathbf{A}-\mathbf{B})}. \tag{8}$$

Due to the inverse of the covariance matrix Σ^{-1}, the MAHALANOBIS distance is weighted by the amount of correlation between $\mathbf{A}$ and $\mathbf{B}$. In this paper, the mean MAHALANOBIS distance

$$\overline{d}_{\mathrm{M}} = \frac{1}{2N}\sum_{i=1}^{N} d_{\mathrm{M}}(\mathbf{A},\mathbf{B}) + \frac{1}{2M}\sum_{i=1}^{M} d_{\mathrm{M}}(\mathbf{B},\mathbf{A}) \tag{9}$$

is used, which is the mean of the bidirectionally calculated MAHALANOBIS distances $d_{\mathrm{M}}(\mathbf{A},\mathbf{B})$ and $d_{\mathrm{M}}(\mathbf{B},\mathbf{A})$.

A zero HAUSDORFF distance or mean MAHALANOBIS distance indicates a perfect agreement, while small distances indicate a high degree of agreement. Higher distances indicate deviations between the measured and the replicated MSTA. However, absolute values for *small* and *high* distances depend on the investigated structures. Thus, the distances only describe the relative degree of agreement of several replicas (or avatars) to each other.

In contrast, the FRFSM measures the degree of agreement on an absolute scale between 0 (no agreement) and 1 (perfect agreement). LEE [11] shows that the FRFSM correlates with the subjective judgment of experts, who rated the degree of agreement of frequency response functions obtained from vibration measurements of passenger cars. In this paper, it is investigated whether the FRFSM can be used to assess the degree of agreement of the replicated MSTA and the measured MSTA as well.

3 EXPERIMENTAL SETUP

Table 1 lists the geometrical dimensions of the rectangular plates that are subject to the experimental investigations of this paper. All plates are manufactured three times and are made from aluminum. The material

properties have been measured for each plate using the method in [7]. The averaged material properties are: YOUNG'S modulus $E = 70.59 \cdot 10^9\,\mathrm{N\,m^{-2}}$, POISSON'S ratio $\mu = 0.33$, and mass density $\rho = 2676\,\mathrm{kg\,m^{-3}}$. A simply supported boundary condition of the rectangular plates is obtained by bonding blades with 0.5 mm thickness to the plates' edges. The blades are clamped to brackets, which are mounted on the test stand. Further details on the design of the simple supported boundary conditions can be found in [4, 6].

Table 1. geometrical dimensions and scaling factors of the rectangular plates; *): calculated according to Eq. (5)

plate		a	b	h	ϕ_a	ϕ_b	ϕ_h	ϕ_l
p	parent	870 mm	620 mm	5.0 mm	1.0	1.0	1.0	1.0
r1	replica	435 mm	310 mm	5.0 mm	0.5	0.5	1.0	0.5
r2	replica	435 mm	310 mm	2.5 mm	0.5	0.5	0.5	0.5
a1	avatar	375 mm	310 mm	5.0 mm	0.43	0.5	1.0	0.466*)
a2	avatar	375 mm	310 mm	2.5 mm	0.43	0.5	0.5	0.466*)

The vibration velocities are obtained from SLDV measurements in the frequency range of 0…5 kHz for one plate of each size as described in [4], and the MSTA is calculated from Eq. (1). The loss factors are measured for all three plates of each size in order to assess the similitude of the damping. Each rectangular plate is excited by an impact and the time-decaying vibrations are measured by an accelerometer. The loss factors of each rectangular plate are obtained at 30 peaks in the vibration spectrum using the 3 dB bandwidth. Further details on the measurement procedure can be found in [3]. The loss factor measurements are performed at three different states: (1) rectangular plates with free boundary conditions, (2) rectangular plates with blades bonded to the edges and free boundary conditions, and (3) rectangular plates with simply supported boundary conditions. This allows for determining the effect of the boundary conditions on the loss factor. In order to analyze the significance of the similitude of the loss factors, an analysis of variance (ANOVA) is performed. Besides the significance of the boundary conditions, the significance of the plates' sizes is analyzed within the ANOVA as well.

4 RESULTS

First, the replicated MSTA is analyzed for all replicas and avatars and the accuracy of the replicated MSTA is qualitatively assessed by a subjective judgment. Second, the results of the loss factor measurements are discussed. Third, the measures defined in Section 2.2 are calculated and the results are discussed.

4.1 Replicating the MSTA

Figure 1 shows the replicated and measured MSTA of the replicas r1 and r2. The replicated MSTA levels agree sufficiently well with the measured ones up to a frequency of approximately 1 kHz. Above 1 kHz, the frequencies with locally increased MSTA levels (peaks) are still accurately replicated, but the replicated MSTA levels themselves tend to be higher than the measured MSTA levels. Since the replicas r1 and r2 are in geometrically complete similitude to the parent, the deviation above 1 kHz is rather caused by an incomplete similitude of the damping than by a geometrically incomplete similitude.

Figure 2 shows the replicated and measured MSTA of the avatars. The MSTA levels agree well at some frequencies, e.g., at approximately 0.9 kHz for avatar a1 or at approximately 0.3 kHz for avatar a2. Due to geometrically incomplete similitude conditions, the vibration behavior of the avatars differs from that of the replicas and, thus, from that of the parent. For example, the replicated MSTA levels of avatar a1 show three peaks between 1.5 kHz and 2.0 kHz that are not shown by the measured MSTA levels.

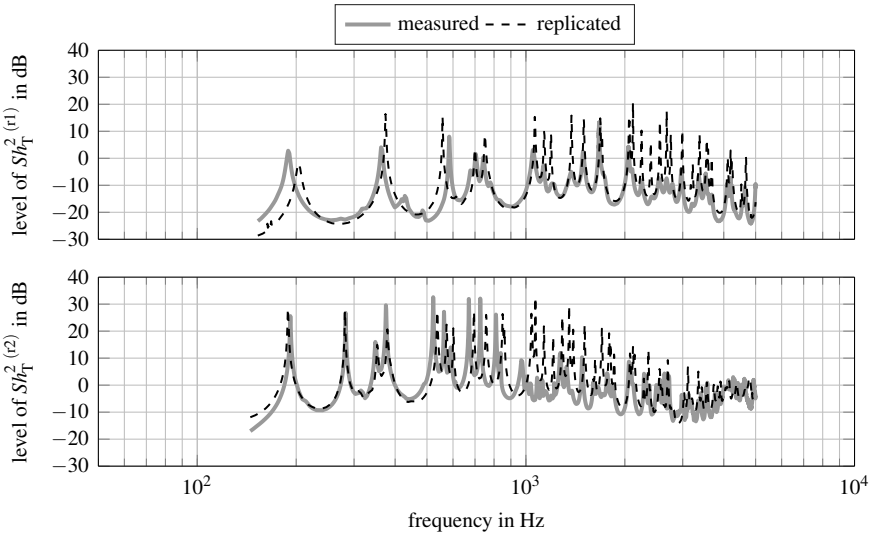

Figure 1. MSTA levels (re $6.25 \cdot 10^{-6}\,\mathrm{m^4\,N^{-2}\,s^{-2}}$) versus frequency of the replicas r1 (top) and r2 (bottom), frequency axis applies to both plots, figure obtained from [3]

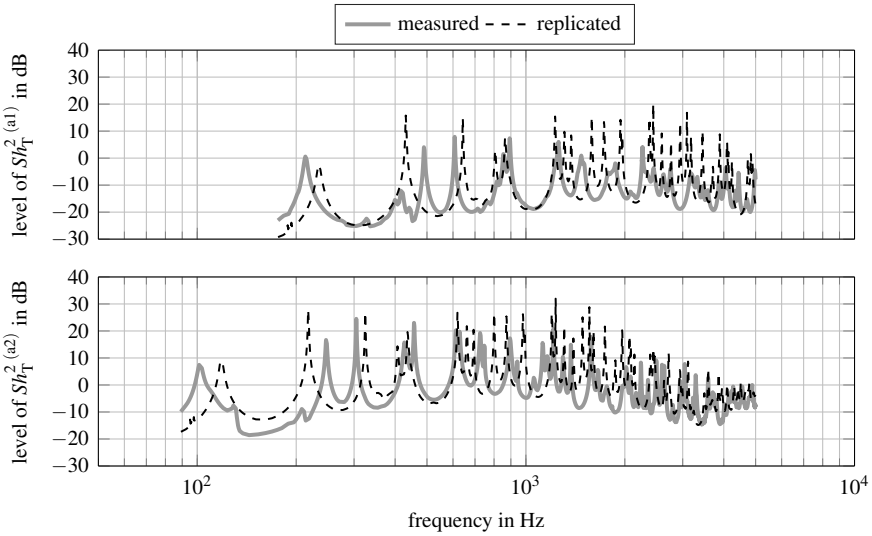

Figure 2. MSTA levels (re $6.25 \cdot 10^{-6}\,\mathrm{m^4\,N^{-2}\,s^{-2}}$) versus frequency of the avatars a1 (top) and a2 (bottom)

The previous analyses of the agreement of the measured and replicated MSTA levels is obtained from visually inspecting Figures 1 and 2, which is a subjective judgment made by the authors of this paper. Other individuals may obtain a different view when analyzing the figures. As a consequence, more objective measures are necessary to assess the agreement between the replicated MSTA and the measured MSTA. Section 4.3 proposes such measures. These measures are analyzed in order to fund out whether they match the subjective judgment of Figures 1 and 2 presented in this section.

4.2 Similitude of the loss factor

The results of the ANOVA are presented as box plots. A detailed analysis can be found in [3]. In this paper, only the main findings are presented. The loss factors are found to be log-normally distributed, which requires the logarithmized loss factors to be used within the ANOVA. It is found that the loss factor significantly increases on a 95% confidence level if the blades are bonded to the plates' edges, which can be seen by the fact that the notches of the boxplot are not overlapping, see Figure 3. The simply supported boundary condition

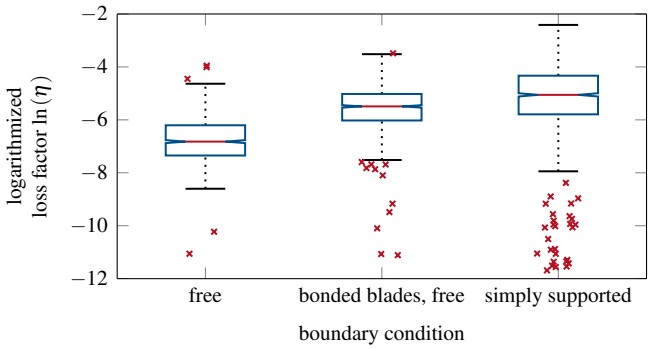

Figure 3. box plot of the logarithmized loss factors subdivided by plates' boundary conditions

yields not only another significant increase of the loss factor on a 95% confidence level, but also causes the variance to increase, which is illustrated by the box' size. As a consequence, the similitude of the loss factors depends on the boundary conditions. Particularly, the simply supported boundary conditions increase the variance of the loss factors, which may lead to an incomplete similitude of the damping and, thus, limits the application of scaling laws in practice. It is shown in [4] that the MSTA levels of rectangular plates in geometrically complete similitude can be replicated sufficiently well if the loss factor is in complete similitude.

Figure 4 shows the box plot of the logarithmized loss factors subdivided by the different plates' sizes. The loss factors significantly differ on a 95% confidence level, while the variance is approximately equal. Thus, the loss factors depend on the plates' sizes as well. Note that this effect is independent from the effect of the boundary conditions, which has previously been described. As a consequence, an incomplete similitude of the loss factors leads to incomplete similitude conditions – even for the rectangular plates in geometrically complete similitude. Thus, the application of scaling laws is limited in practice and incomplete similitude causes the replicated MSTA levels to differ from the measured ones as can be seen in Figures 1 and 2. In order to find the limits of the application of scaling laws, it is necessary to assess the agreement of the measured and the replicated MSTA, which requires appropriate measures. Such measures are analyzed in Section 4.3.

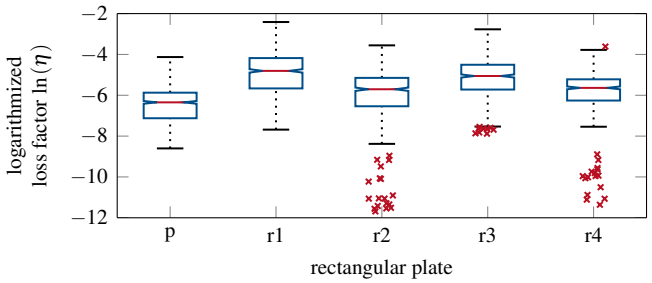

Figure 4. box plot of the logarithmized loss factors subdivided by plates' sizes

4.3 Assessing the similitude

The results in Section 4 show that

1. analyzing the agreement between replicated MSTA and measured MSTA is somewhat subjective, and
2. limitations of the application of scaling laws arise from the fact that complete similitude conditions are hardly fulfilled in practice.

However, both findings lead to the fact that the *degree of agreement* between replicated MSTA and measured MSTA needs to be assessed. Therefore, d_H, $\overline{d}_\mathrm{M}$, and the FRFSM are calculated using the measured and the replicated MSTA of each replica and avatar. As discussed in Section 4.1, the MSTA of the replicas r1 and r2 subjectively agree well below 1 kHz. Thus, d_H, $\overline{d}_\mathrm{M}$, and the FRFSM are not only calculated over the entire frequency range $0\ldots5$ kHz, but also for $0\ldots1$ kHz and $>1\ldots5$ kHz.

Table 2 shows the results. Considering the entire frequency range the mean MAHALANOBIS distance $\overline{d}_\mathrm{M}$ and the FRFSM match the subjective judgment by the authors for the replicas, since the mean MAHALANOBIS distance $\overline{d}_\mathrm{M}$ (the FRFSM) of replica r1 is higher (lower) than that of replica r2. Based on the subjective judgment it has been concluded that the replicated MSTA agrees well with the measured MSTA below 1 kHz for the replicas r1 and r2 (see Section 4.1), while the MSTA agrees to a lesser extent above 1 kHz. The HAUSDORFF distance and the FRFSM reflect this subjective judgment, since the HAUSDORFF distances and the FRFSM in the frequency range $0\ldots1$ kHz of the replicas r1 and r2 are smaller than those in the frequency range $>1\ldots5$ kHz. In case of the avatars, the HAUSDORFF distance, the mean MAHALANOBIS distance, and the FRFSM do not generally show that the MSTA agrees to a lesser extent than the MSTA of the replicas. For example, the mean MAHALANOBIS distance equals $4.36\cdot10^{-3}\,\mathrm{m^4\,N^{-2}\,s^{-2}}$ and $0.44\cdot10^{-3}\,\mathrm{m^4\,N^{-2}\,s^{-2}}$ in the frequency range $0\ldots5$ kHz for the replica r2 and the avatar a2, respectively, which indicates that the replicated and measured MSTA agree well for avatar a2, while they (somewhat) deviate for replica r2. However, the subjective judgment (see Section 4.1) yields a different result.

Table 2. measures to assess the degree of agreement of the MSTA, d_H and $\overline{d}_\mathrm{M}$ are given in $\mathrm{m^4\,N^{-2}\,s^{-2}}$, while FRFSM is dimensionless

	$0\ldots5$ kHz			$0\ldots1$ kHz			$>1\ldots5$ kHz		
plate	d_H	$\overline{d}_\mathrm{M}$	FRFSM	d_H	$\overline{d}_\mathrm{M}$	FRFSM	d_H	$\overline{d}_\mathrm{M}$	FRFSM
r1	$0.15\cdot10^{-3}$	$11.91\cdot10^{-3}$	0.18	$0.06\cdot10^{-3}$	$10.50\cdot10^{-3}$	0.54	$0.15\cdot10^{-3}$	$18.72\cdot10^{-3}$	0.11
r2	$6.60\cdot10^{-3}$	$4.36\cdot10^{-3}$	0.32	$10.34\cdot10^{-3}$	$238.16\cdot10^{-3}$	0.43	$1.16\cdot10^{-3}$	$138.52\cdot10^{-3}$	0.30
a1	$0.15\cdot10^{-3}$	$107.24\cdot10^{-3}$	0.21	$0.02\cdot10^{-3}$	$2.39\cdot10^{-3}$	0.45	$0.25\cdot10^{-3}$	$1661.40\cdot10^{-3}$	0.16
a2	$2.50\cdot10^{-3}$	$0.44\cdot10^{-3}$	0.30	$0.77\cdot10^{-3}$	$12.74\cdot10^{-3}$	0.37	$2.50\cdot10^{-3}$	$0.42\cdot10^{-3}$	0.28

5 CONCLUSIONS

Scaling laws derived from numerical calculations are applied in order to replicate the measured MSTA of simply supported rectangular plates in geometrically complete and incomplete similitude. An ANOVA of the loss factors shows that rectangular plates are not in complete similitude regarding the damping, which is caused by the simply supported boundary conditions and by the plates' sizes themselves. Both incomplete similitude due to the damping and geometrically incomplete similitude cause the replicated MSTA to deviate from the measured MSTA.

The HAUSDORFF distance, the mean MAHALANOBIS distance, and the FRFSM are used to assess how well the scaling laws replicate the measured MSTA. These measures match the subjective judgment of the agreement of the replicated and measured MSTA in some cases, while they are contradictory to the subjective judgment

in other cases. Further research will, thus, focus on developing an improved measure to determine the *degree of agreement*. Such an improved measure should reliably turn the subjective judgment of individuals into an objective figure. Thus, judging of the agreement of the MSTA (or frequency response functions in general) by individuals needs to be understood in more detail.

ACKNOWLEDGEMENTS

The authors acknowledge the financial support for the scanning laser DOPPLER vibrometer from Deutsche Forschungsgemeinschaft (DFG) under grant number INST 163/520-1.

REFERENCES

[1] Casaburo, A.; Petrone, G.; Franco, F.; De Rosa, S. A review of similitude methods for structural engineering. Applied Mechanics Reviews, 71(3), 2019, 030802-1–030802-32.

[2] Adams, C.; Bös, J.; Slomski, E.M.; Melz, T. Scaling laws obtained from a sensitivity analysis and applied to thin vibrating structures. Mechanical Systems and Signal Processing, 110, 2018, 590–610.

[3] Adams, C. Similitudes and sensitivities as contributions to scaling laws in machine acoustics. PhD dissertation, Technische Universität Darmstadt, Darmstadt, Germany, 2019.

[4] Adams, C.; Bös, J.; Melz, T. An experimental investigation of vibrating plates in similitude and the possibility to replicate the responses using sensitivity-based scaling laws. In 6th NOVEM – Noise and Vibration Emerging Methods, Ibiza, Spain, May 07–09, 2018.

[5] De Rosa, S.; Franco, F. Analytical similitudes applied to thin cylindrical shells. Advances in Aircraft and Spacecraft Science, 2(4), 2015, 403–425.

[6] Robin, O.; Chazot, J.D.; Boulandet, R.; Michau, M.; Berry, A.; Atalla, N. A plane and thin panel with representative simply supported boundary conditions for laboratory vibroacoustic tests. Acta Acustica united with Acustica, 102(1), 2016, 170–182.

[7] Langer, P.; Sepahvand, K.; Guist, C.; Bär, J.; Peplow, A.; Marburg, S. Matching experimental and three dimensional numerical models for structural vibration problems with uncertainties. Journal of Sound and Vibration, 417, 2018, 294–305.

[8] Huttenlocher, D.P.; Klanderman, G.A.; Rucklidge, W.J. Comparing images using the Hausdorff distance. IEEE Transactions on Pattern Analysis and Machine Intelligence, 15(9), 1993, 850–863.

[9] Meruane, V.; De Rosa, S.; Franco, F. Numerical and experimental results for the frequency response of plates in similitude. Proceedings of the Institution of Mechanical Engineers, Part C: Journal of Mechanical Engineering Science, 230(18), 2016, 3212–3221.

[10] Mahalanobis, P.C. On the generalized distance in statistics. Proceedings of the National Institute of Sciences of India, 2(1), 1936, 49–55.

[11] Lee, D.; Ahn, T.S.; Kim, H.S. A metric on the similarity between two frequency response functions. Journal of Sound and Vibration 436, 2018, 32–45.